Published in final edited form as:
Neurobiol Dis. 2009 May ; 34(2): 267–278. doi:10.1016/j.nbd.2009.01.013.

Anti-PrP Mab 6D11 suppresses PrP^{Sc} replication in prion infected myeloid precursor line FDC-P1/22L and in the lymphoreticular system in vivo

Martin J. Sadowski[a,b,c,*], **Joanna Pankiewicz**[a], **Frances Prelli**[a], **Henrieta Scholtzova**[a], **Daryl S. Spinner**[e], **Regina B. Kascsak**[e], **Richard J. Kascsak**[e], and **Thomas Wisniewski**[a,b,d,e,*]

[a]Department of Neurology, New York University School of Medicine, 550 First Avenue, New York, NY 10016, USA

[b]Department of Psychiatry, New York University School of Medicine, 550 First Avenue, New York, NY 10016, USA

[c]Department of Pharmacology, New York University School of Medicine, 550 First Avenue, New York, NY 10016, USA

[d]Department of Pathology, New York University School of Medicine, 550 First Avenue, New York, NY 10016, USA

[e]New York State Institute for Basic Research in Developmental Disabilities, 1050 Forest Hill Road, Staten Island, NY 10314, USA

Abstract

The pathogenesis of prion diseases is related to conformational transformation of cellular prion protein (PrP^{C}) into a toxic, infectious, and self-replicating conformer termed PrP^{Sc}. Following extracerebral inoculation, the replication of PrP^{Sc} is confined for months to years to the lymporeticular system (LRS) before the secondary CNS involvement results in occurrence of neurological symptoms. Therefore, replication of PrP^{Sc}, in the early stage of infection can be targeted by therapeutic approaches, which like passive immunization have limited blood-brain-barrier penetration. In this study, we show that 6D11 anti-PrP monoclonal antibody (Mab) prevents infection on a FDC-P1 myeloid precursor cell line stably infected with 22L mouse adapted scrapie strain. Passive immunization of extracerebrally infected CD-1 mice with Mab 6D11 resulted in effective suppression of PrP^{Sc} replication in the LRS. Although, a rebound of PrP^{Sc} presence occurred when the Mab 6D11 treatment was stopped, passively immunized mice showed a prolongation of the incubation period by 36.9% ($p<0.0001$) and a significant decrease in CNS pathology compared to control groups receiving vehicle or murine IgG. Our results indicate that antibody-based therapeutic strategies can be used, even on a short-term basis, to delay or prevent disease in subjects accidentally exposed to prions.

*Corresponding authors. M.J. Sadowski is to be contacted at New York University School of Medicine, 550 First Ave., PRR, Rm. RR 311, New York, NY10016, USA. Fax:+1212 263 7721. T. Wisniewski, New York University School of Medicine, Millhauser Laboratory, Room HN419, 550 First Avenue, New York, NY 10016, USA. Fax: +1 212 263 7528. *E-mail addresses*: E-mail: sadowm01@med.nyu.edu (M.J. Sadowski), thomas. E-mail: wisniewski@med.nyu.edu (T. Wisniewski).

Disclosure statement

All authors have no actual or potential conflicts of interest regarding the work described in this manuscript to disclose. In particular, there are no conflicts of interest including any financial, personal or other relationships with other people or organizations within three years of beginning the work submitted that could inappropriately influence (bias) their work.

Keywords

Monoclonal antibodies; Scrapie; Neuroinvasion; Prion; Treatment; Creutzfeldt–Jakob

Introduction

Prion diseases (prionoses) are transmissible, invariably fatal, neurodegenerative diseases associated with a conformational transformation of cellular prion protein PrP^{C} into a toxic, infectious, and self-replicating PrP^{Sc} conformer for which noeffective treatment is currently available (Prusiner, 2001; Sadowski et al., 2008; Weissmann, 2004). Accidental prion infection in humans may occur as a result of consumption of food products derived from cattle infected with bovine spongiform encephalopathy (BSE), disease transmission from other humans who have already contracted the human BSE homolog variant Creutzfeldt–Jakob disease (vCJD), but have not yet developed clinical symptoms, or from patients with sporadic CJD who are in preclinical or unrecognized clinical stagesofthe disease (Brown et al., 2006; Sadowski et al., 2008). During the initial stage of extracerebral prion infection, replication of PrP^{Sc} is supported by several lymphoid cell lineages which are associated with accumulation of PrP^{Sc} in the lymporeticular system (LRS) organs (Aucouturier et al., 1999; Liu et al., 2001; Mabbott and MacPherson, 2006). Replication of PrP^{Sc} on lymphoid cells may take month to years before secondary CNS involvement and occurrence of clinical symptoms (Eklund et al.,1967; Hilton et al., 2004b; Mabbott and MacPherson, 2006; Rubenstein et al., 1991). During this period, asymptomatic vCJD carriers constitute a reservoir of infection. It is estimated that more than 10,000 Britons could be vCJD infected as a result of BSE exposure during the early 90s epidemics, yet remain asymptomatic carriers of prionoses (Hilton et al., 2004a; Hilton, 2006).

The four possible cases of disease transmission related to blood transfusion donated by asymptomatic individuals infected with vCJD, published so far, justify clinical concerns of more wide spread blood bank contamination (Llewelyn et al., 2004; Peden et al., 2004; Wroe et al., 2006). In addition to transmission via blood transfusion and organ transplantation, human to human transmission may also occur via infectious material transferred by surgical (especially neuro-surgical) (Weissmann et al., 2002) or dental tools (Porter, 2003) and endoscopic instruments since PrP^{Sc} is known to accumulate in the intestinal mucosa of asymptomatic BSE-infected carriers (Prinz et al., 2003; Wadsworth et al., 2001).

Since no effective treatment for prion diseases exists, development of therapeutic approaches for this group of universally fatal diseases is a priority. Reports from several laboratories including our own have demonstrated that selected anti-PrP Mabs can permanently abrogate the presence of PrP^{Sc} from murine neuroblastoma and hypothalamic cell lines infected with mouse adapted scrapie strains rendering these lines noninfectious (Enari et al., 2001; Feraudet et al., 2005; Pankiewicz et al., 2006; Peretz et al., 2001; Perrier et al., 2004). Therefore, passive immunization with anti-PrP Mabs possessing therapeutic properties could constitute a viable strategy to target PrP^{Sc} replication on the lymphoid cells with the aim to prevent prion neuroinvasion and occurrence of neurological symptoms. It has been demonstrated that several lymphoid cell lineages including B and T lymphocytes (Liu et al., 2001; Montrasio et al., 2001; Weissmann et al., 2001), bone marrow progenitor cells (Liu et al., 2001), macrophages (Prinz et al., 2002), dendritic cells (Aucouturier et al., 2001; Burthem et al., 2001), splenocytes (Parizek et al., 2001) and follicular dendritic cells (FDCs) (Brown et al., 1999; Weissmann et al., 2001) show transient or permanent expression of PrP^{C}. Expression of PrP^{C} appears to be particularly abundant during the development of some of these lineages and thus PrP^{C} has been implicated in the process of hematopoietic differentiation and maturation (Liu et al., 2001). With the aim to establish a model of peripheral PrP^{Sc} replication we have successfully infected

a factor dependant P1 cell line (FDC-P1) with 22L mouse adapted scrapie strain. FDC-P1 is representative of a murine myeloid hematopoietic precursor clone (Bourette et al., 1995; Dexter et al., 1980) It expresses a significant amount of PrP^{C} and is capable of self-renewal in the presence of interleukin-3 and thus can be used for modeling of prion infection in vitro (Bourette et al.,1995; Dexter et al., 1980). Thus far, the therapeutic effect of anti-PrP has not been characterized in lymphoid cells. We have used the stably infected line FDC-P1/22L line to characterize the therapeutic effect of anti-PrP Mab 6D11, which recognizes both murine and human PrP (Spinner et al., 2007) and has previously demonstrated its therapeutic effect in prion infected N2a/22L murine neuroblastoma line (Pankiewicz et al., 2006). Following demonstration that 6D11 abrogates the presence of PrP^{Sc} from infected FDC-P1/22L cells we tested the effect of passive immunization with this Mab on replication of PrP^{Sc} in the LRS in extracerebrally infected mice. We report here that systemic administration of 6D11 results in suppression of PrP^{Sc} replication in the lymphoid organs akin to the effects observed in vitro although PrP^{Sc} replication rebounded after cessation of treatment. Nevertheless, short-term passive immunization had a significant effect on delaying the clinical onset of disease and produced a reduction of brain pathology due to impaired neuroinvasion.

Methods

Monoclonal antibodies

Development and characterization of the Mab 6D11 was reported previously (Pankiewicz et al., 2006; Spinner et al., 2007). Briefly, Mab 6D11 was raised against nondenaturated scrapie-associated fibrils that were purified using proteinase K (PK) treatment from brains of terminally ill CD-1 mice infected with 139A strain (Kascsak et al., 1987). The immunization was performed in $Prnp^{0/0}$ mice using TiterMax and the TLR9 agonist CpG oligodeoxynucleotide 1826 together as adjuvants. The epitope of 6D11 was mapped to residues 97–100 of murine PrP (Q W N K; see Fig. 1B) (Spinner et al., 2007). Since the sequence of murine PrP residues 97–100 is identical with residues, 98–101 of human PrP it is likely that 6D11 recognizes human PrP as well. Therefore, we used Western-blot and ELISA to compare the reactivity of Mab 6D11 and Mab 3F4, which is known to react with human PrP (residues 109–112) but not with murine PrP (Kascsak et al.,1987,1986). We compared the reactivity of both Mabs against brain samples from patients with Gerstmann–Sträussler–Scheinker (GSS) syndrome, sporadic CJD, Alzheimer's disease (AD), and normal controls. The PK digestion and Western-blotting of human brain samples were performed exactly as described below for brains of mice treated with Mab 6D11. Samples of human brains were obtained from the Brain Bank of the New York University Alzheimer's Disease Clinical Center. We used ELISA to compare the binding affinities of these two Mabs torecombinant murine and human PrP. ELISA was performed on Immulon 2HB plates (Thermo Fisher Scientific Inc. Waltham, MA) coated with 50 ng/well of either murine or human recombinant PrP as previously described (Pankiewicz et al., 2006; Spinner et al., 2007). Briefly, after washing and blockingof unbounded sites with SuperBlock (Pierce, Rockford, IL) titration series of 6D11 and 3F4 Mabs ranging from 0 to 6.7 nM (1 mg/ml) were added and followed by subsequent incubation with anti-mouse IgG HRP-conjugate (Amersham Bio-sciences; Piscataway, NJ) at 1:5000 in PBST at 37 °C for 1 h and 3,3,5,5-tetramethybenzidine substrate (TMB; Sigma, St. Louis, MO). Optical density (OD) values were analyzed with an one site binding nonlinear regression fit algorithm using GraphPad Prism v4.0 (GraphPad Software, San Diego, CA).

For passive immunization experiments large quantities of Mab 6D11 were obtained by culturing the corresponding hybridoma line in INTEGRA CL bioreactor flasks (BD Biosciences, Bedford, MA). Mab 6D11 was purified using Pierce Ultra-Link Immobilized Protein A/G Plus affinity resin (Pierce; Rockford, IL), and the concentration was determined

using a mouse IgG radial immunodiffusion assay kits (MP Biomedicals; Irvine, CA). Control murine IgG was obtained from Sigma-Aldrich (St. Louis, MO).

Characterization of PrP^C expression in FDC-P1 line and infection with 22L strain

FDC-P1 line (CRL-12103) was obtained from American Type Culture Collection (ATCC, Manassas, VA). FDC-P1 line is a murine myeloid hematopoietic precursor clone established from the long-term culture of DBA/2 bone marrow cells grown in medium conditioned by WEHI-3 cells producing macrophage colony stimulating factor (Dexter et al., 1980; Junttila et al., 2003). FDC-P1 cells were maintained in 12.5 cm^2 flasks in Dulbecco's Modified Eagle's Medium supplemented with L-glutamine (4 mM), heat-deactivated 10% fetal bovine serum (FBS), interleukin-3 (5 ng/L; Sigma-Aldrich, St. Louis, MO), penicillin (100 U/mL) and streptomycin (100 μg/mL) at 37 °C in 5% CO_2. Expression of PrP^C in FDC-P1 line was confirmed by Western-blotting and immunohistochemistry. For Western-blotting FDC-P1 cells were harvested using ice cold lysis buffer (150 mM NaCl, 0.5% triton X-100, 0.5% sodium deoxycholate and50mMTris–HCL pH7.5 with Complete® protease inhibitor (Boehringer-Mannheim, Indianapolis IN) and centrifuged for 3 min at 10,000 ×g to remove cell debris. The total protein concentration was measured in the supernatant using the bicinchoninic acid assay (BCA, Pierce; Rockford, IL). Samples of supernatant containing varying amounts of total protein were subjected to SDS-PAGE and Western transfer as previously described (Jimenez-Huete et al., 1998; Pankiewicz et al., 2006). Membranes were probed with Mab 6D11 (0.05 μg/ml) followed by a horseradish-peroxidase (HRP) conjugated sheep anti-mouse antibody at a dilution of 1:5000 (Amersham Biosciences; Piscataway, NJ) and developed using a chemiluminescent reagent (SuperSignal; Pierce, Rockford, IL).

For immunohistochemical detection of PrP, cells were cultured on coverslips and fixed with 20% ice-cold methanol. PrP was detected with Mab 6D11 followed by biotinylated secondary anti-mouse IgG antibody and avidin-FITC complex (Vector Laboratories, Ltd., Vector Burlingame, CA). Cells were counterstained with DAPI (4′,6′-diamidino-2-phenylindole dihydrochloride) and analyzed under a deconvolution fluorescence microscope Zeiss Axioskop 40 (Carl Zeiss AG, Gottingen, Germany) or a Bio-Rad (Hercules, CA, USA) Radiance 2000 confocal system attached to the Olympus BX50WI fluorescence microscope.

The FDC-P1 line was infected with 22L PrP^{Sc} strain during a 22 hour exposure to a 4% brain homogenate from terminally sick animals as described previously (Pankiewicz et al., 2006). Within 24–48 h following the infection cells were split 1:2 and grown in 12.5 cm^2 flasks until approximate confluence. Then the first flask was split again 1:2 to give rise to subsequent passages, whereas cells grown in the second flask were harvested to assess the level of PrP^{Sc}. To increase the rate of infectivity during exposure of FDC-P1 cells to 22L brain homogenate and subsequently to maintain the infected line, the flasks containing FDC-P1 cells were constantly kept on a rocker (Rocker 25 Labnet Int. Woodbridge NJ) that was placedinthe cell culture incubator. Since FDC-P1 cells grow as a suspension, constant movement of the medium increases cell contacts and cell-to-cell transmission of PrP^{Sc}. The RAW 264.7 murine macrophage line (ATCC line CRL-2278) was used as a negative control in the infection experiment since these cells engulf PrP^{Sc}, but have no capabilityof sustaining PrP^{Sc} replication (Luhr et al., 2002). RAW 264.7 cells were grown in RPMI-1640 medium supplemented with 2 nM L-glutamine, 10% FBS, penicillin and streptomycin. They were infected with 4% 22L brain homogenate analogous to the FDC-P1 cells. Murine neuroblastoma N2a cells (ATCC line CCL 131) were grown in the Minimal Essential Medium supplemented with 10% FBS, penicillin and streptomycin and infected with 2% 22L brain homogenate as described previously (Pankiewicz et al., 2006). The level of PrP^{Sc} in the subsequent passages following infection was determined by PK digestion and Western-blot analysis as previously described (Pankiewicz et al., 2006). Briefly, aliquots of cell lysates containing 200 μg of total protein

were titrated by adding buffer to achieve a final protein concentration of 1 μg/μl. PK digestion (Roche; Indianapolis, IN) was performed for 30 min at 37 °C maintaining the enzyme to protein weight ratio 1 to 50 (Perrier et al., 2004). PK activity was quenched by adding phenylmethylsulfonyl fluoride (PMSF). Samples were then centrifuged at 14,000 ×g for 45 min at 4 °C and pellets were resuspended in 15 μl TBS and 15 μl sample buffer containing 2-mercaptoethanol, boiled for 5 min, and then subjected to SDS-PAGE electrophoresis followed by transfer onto nitrocellulose membranes (Amersham Biosciences; Piscataway, NJ), which were probed with Mab 6D11 (0.05 μg/ml) and developedas described above. In each assay, three samples of non-infected cells were used as a negative control to assure complete PK digestion of PrP^{C}.

Treatment of FDC-P1/22L and N2a/22L lines with Mab 6D11

Two types of treatment experiments were performed. First, we tested whether Mab 6D11 can prevent the infection of FDC-P1 cells. FDC-P1 cells were cultured overnight in the media supplemented with 10 μg/ml of Mab 6D11 and after washing with PBS, the cells were infected with 4% 22L brain homogenates as described above. In parallel experiment 22L brain homogenates were diluted in medium to a final concentration of 4% and incubated with 40 μg of 6D11/mL for 2 h prior to addition to the cells. The level of PrP^{Sc} was assessed in subsequent passages using PK digestion and Western-blot analysis as described above and compared to FDC-P1 cells infected with 22L in the absence of 6D11. Non-infected FDC-P1 cells were used as a negative control to assure complete PK digestion of PrP^{C}.

In the experiment designed to test whether Mab 6D11 can abrogate the presence of PrP^{Sc} from already infected FDC-P1 cells (FDC-P1/22L) the fourth passage of infected cells was incubated with increasing concentrations of Mab 6D11 (0–10 μg/mL) for 96 h. We used the fourth passage to assure that detected PrP^{Sc} is derived from de novo conversion of native PrP^{C} to PrP^{Sc} and does not represent PrP^{Sc} carried over from the inoculum. Infected N2a line (N2a/22L) was used for comparison. The level of PK resistant PrP^{Sc} following the treatment was determined densitometrically on Western-blot as described below. It was expressed as a percent of the average value for untreated FDC-P1/22L or N2a/22L cells considered as 100%. The half of maximal inhibitory concentration ($IC_{50\%}$) was determined by fitting the data into a sigmoidal dose–response curve using Graph Pad Prism Software v4.03 (Graph Pad Prism Software, Inc., San Diego, CA, USA).

A colorimetric MTT (3-[4,5-dimethylthiazol-2-yl]2,5-diphenylte-trazolium bromide) assay (Roche, Indianapolis, IN) was performed to assess the viability of prion infected FDC-P1 cells undergoing treatment with 6D11 Mab (Pankiewicz et al., 2006; Sadowski et al., 2004). FDC-P1 and infected FDC-P1/22L cells were cultured in 96-well microtiter plates in the presence of 6D11 or murine IgG (Sigma-Aldrich, St. Louis, MO) at a concentration of 10 μg/ml for 96 h and then the viability of cells was assessed using a MTT kit according to the manufacturer's instructions.

Passive immunization of CD-1 mice with Mab 6D11 following inoculation with prions

We tested the effect of short-term systemic passive immunization with 6D11 Mab on the accumulation of PrP^{Sc} in the LRS and on the length of the incubation period. Three-months old female CD-1 mice were inoculated by a single intraperitoneal injection of 100 μl of 10% brain homogenate from terminally ill mice infected with 22L mouse adapted scrapie strain. All animals were inoculated from a single batch of 22L inoculum prepared from a pool of brains harvested under sterile conditions. This is a well-established model of prion disease in mice, which leads to neurological symptoms around 150 days post inoculation (dpi) and death in all cases, if the disease is allowed to progress (Aucouturier et al., 2001; Carp et al., 1984; Kimberlin and Walker, 1989; Sigurdsson et al., 2002). The experimental design included six groups of

20 animals each, which received Mab 6D11, murine IgG, or vehicle (PBS) for either four or eight weeks. Within an hour of inoculation mice received a single 1 mg dose of 6D11 Mab (in 200 µl PBS) intravenously which was followed by intraperitoneal injections of 0.5 mg of 6D11 (in 200 µl PBS) twice a week. Control groups received equivalent doses of murine IgG or vehicle. Dosing was established based on previous studies (Sigurdsson et al., 2003; White et al., 2003). When treatment was completed (i.e after four or eight weeks) five animals from each group (sentinel mice) were sacrificed and tested for the presence of PrP^{Sc} in the spleen and in the brain using a highly sensitive immunoblotting assay (HSIBA). HSIBA provides enhanced sensitivity of PrP^{Sc} detection, by the precipitation of PrP^{Sc} with sodium phosphotungstic acid (NaPTA) prior to PK digestion (Safar et al., 1998; Wadsworth et al., 2001; White et al., 2003). Briefly, 100 µl aliquots of 10% (w/v) spleen or brain homogenates were mixed with 4% sarcosyl in PBS and incubated for 10 min at 37 °C. Then 50 U/mL of Benzonase (Benzon nuclease, purity 1, Merck) was added and samples were adjusted to 1 mmol/L $MgCl_3$ and incubated for 30 min at 37 °C. A solution of 4% NaPTA,170 mmol/L $MgCl_3$, pH 7.4 was added to samples to obtain a final concentration of 0.3% NaPTA and samples were incubated at 37 °C for 30 min with constant agitation, and then centrifuged at 15,800 ×g for 30 min. The pellet was re-suspended in 200 µl of 0.1% sarcosyl in PBS pH 8.0 and centrifuged at 15,800 ×g for 15 min. The final pellet was subjected to PK digestion, SDS-PAGE and Western transfer. Membranes were probed with Mab 7A12 (1:1000) which binds to a different epitope than that of 6D11 (Pankiewicz et al., 2006; Zanusso et al., 1998) to avoid possibility that lack of PrP^{Sc} detection in 6D11 treated mice is a result of epitope masking.

The remaining 15 mice in each group were kept alive and monitored for early neurological signs starting from the 100th dpi using a parallel bar crossing test. This task involves assessment of the mouse's competency to cross a series of parallel bars that are 3 mm in diameter and are placed 7 mm apart (Goni et al., 2005; Sadowski et al., 2003; Sigurdsson et al., 2002,2003). The earliest detectable clinical symptoms of CNS involvement include an impaired level of activity and competency when the mouse attempts to cross the parallel bars. The test was administered weekly by a single tester (H.S.) blinded to the animal's treatment group assignment. An animal was considered clinically symptomatic if it scored positive for disease for three consecutive weeks. All animals were euthanized at the same early clinical stage of the disease (following three positive evaluations). All animal experiments were performed according to a protocol approved by the New York University School of Medicine Institutional Animal Care and Use Committee.

Euthanasia, organ harvesting, histological and biochemical tissue processing

Animals were euthanized using an ip. injection of sodium pentobarbital (150 mg/kg) and perfused with heparinized PBS. Spleens and brains were collected and divided for histological and biochemical analysis. The right brain hemisphere and half of the spleen were fixed by overnight immersion in 4% paraformaldehyde, dehydrated in increasing concentrations of ethanol, cleared in xylene, and embedded in paraffin. Eight-micrometer-thick, serial frontal sections were cut using a rotary microtome. Spleen sections were stained with hematoxylin-eosin, Mallory iron stain and 7A12 Mab (1:1000). The anti-PrP immunohistochemistry was performed on sections treated with 44% formic acid (Sigma-Aldrich, St. Louis MO) for 15 min using a mouse-on-mouse kit (Vector Laboratories, Burlingame, CA). Brain sections were stained with hematoxylin-eosin and anti-glial fibrillary acid protein (GFAP) immunohistochem-istry (1:800, Sigma-Aldrich, St. Louis, MO). The numerical density of spongiform changes in the neocortex was quantified using Bioquant NovaPrime v. 6.95 image analysis system (R&M Biometrics Inc., Nashville TN) on sections stained with hematoxylin-eosin. The analysis was performed on ten consecutive cross-section profiles of the cortex separated by 600 µm using a systematic, random sampling scheme free of operator-driven bias which allows maintaining the coefficient of error below 0.06 (West et al., 1991).

Samples designated for biochemical analysis were immediately weighed, homogenized and sonicated (10% w/v) in a buffer containing 20 mM Tris pH 7.5, 250 mM sucrose,1 mM EDTA, 1 mM EGTA, and Complete® protease inhibitor (Boehringer-Mannheim, Indianapolis IN). Samples were centrifuged for 3 min at 10,000 ×g at 4 °C to remove cellular debris the total protein concentration was assayed by the BCA method as described above. If not used immediately, supernatants were divided into 100 µl aliquots, which were flash frozen and stored at −80 °C. Semi-quantitative Western-blot was used to compare the relative content of PrP^{Sc} among samples containing matched amounts of total protein. Aliquots of brain homogenates containing 20 µg of the total proteins and aliquots of spleen homogenates containing 40 µg of total protein, were titrated by adding buffer to a final protein concentration of 1 µg/1 µl. Samples were subjected to PK digestion, SDS-PAGE and Western-blotting into nitrocellulose membranes where PK-resistant PrP^{Sc} was detected with Mab 6D11 (0.05 µg/ml) as described above. In each PK assay at least two samples of brain and spleen from non-infected animals were included as controls to assure that PK sensitive PrP^{C} was completely digested.

For semi-quantification of GFAP level, brain homogenates containing 5 µg of total protein were re-suspended in 15 µl PBS and 15 µl sample buffer, boiled for 5 min, then subjected to SDS-PAGE and transfer onto nitrocellulose membranes as described above. GFAP was detected using anti-GFAP Mab (1:5000; Sigma-Aldrich, St. Louis, MO).

Densitometric analysis of Western-blot signal

For the densitometric analysis, the exposure time of Western-blot membranes was kept standard in all experiments at 30 s. Developed films were converted into 8 bit grayscale digital files using a Epson Perfection 4990 scanner (Epson America; Long Beach, CA) and Adobe Photoshop software 7.01 (Adobe Systems; San Jose, CA) and saved in a TIF format with a resolution of 600 dpi. Quantification of PrP^{Sc} and GFAP were performed using NIH Image J software v 1.34. Areas under the curves for three PrP bands representing non-, mono-, and diglycosylated isoforms of the protein were summarized from each sample to calculate the total PrP level. Analogously, areas under the curves for the two GFAP bands, the main 55 kDa band and the secondary 48 kDa band were summarized to calculate the total GFAP level.

Statistical and power analysis

The measurable outcome in the passive immunization experiment was the length of incubation period defined as the number of days between the day of inoculation and occurrence of the first clinical symptoms (not the time when animals were sacrificed which was 21 days later). It was analyzed using the Kaplan–Meier survival analysis and differences between groups were compared using log– rank test. Design of the passive immunization experiment involved statistical power analysis to determine the most efficient number of animals per group. We determined that for log–rank test having 15 animals per group would be sufficient to maintain the 80% power at α=0.05 while detecting difference >6% between groups.

Differences in quantified measures of brain pathology including the numerical density of spongiform changes, levels of PrP^{Sc} in the spleen and in the brain, and the level of GFAP in the brain were analyzed using one-way ANOVA followed by a Tukey-HSD post-hoc test. Again prior to commencing the experiment we determined that with n = 15 per group, α<0.05 and power >80% the smallest detectable difference between groups for a one-way ANOVA shall be >7%. The statistical and power analyses were performed using Graph Pad Prism Software v4.03 (Graph Pad Prism Software, Inc., San Diego, CA, USA) and CSS Statistica v6 (StatSoft, Inc. Tulsa, OK).

Results

Mab 6D11 equally recognizes murine and human PrP^{Sc}

Mab 6D11 showed strong reactivity with PK digested samples from a brain of sporadic CJD patient and a brain of CD-1 mice infected with 139A strain (Fig. 1A). Mab 6D11 also reacted with a PK digested sample from a brain of GSS syndrome patient. There was no reactivity with PK treated samples of normal human, AD, and normal murine brains indicating complete digestion of PrP^{C} by PK. The well described Mab 3F4 (Kascsak et al., 1987,1986), which binds to human but not to the murine PrP sequence was used for comparison. Reactivity of Mab 3F4 with PK digested samples from GSS and sporadic CJD cases was comparable to that of Mab 6D11. Unlike Mab 6D11, Mab 3F4 did not react with PK-resistant murine PrP from a mouse infected with 139A strain (Fig. 1A). Fig. 1B shows a comparison of the murine and human PrP sequences. Mab 6D11 recognizes epitope QWNK which corresponds to residues 97–100 of murine PrP and residues 98–101 of human PrP. The binding affinity of Mab 6D11 to murine and human recombinant PrP showed similar affinities: $8.5\pm 0.18\times10^{-11}$ M vs. $10.1 \pm0.09\times10^{-11}$ M, respectively (Fig. 1C). These values were comparable to the binding affinity of 3F4 Mab to the recombinant human PrP $16.5\pm0.08\times10^{-11}$ M. As previously described 3F4 did not bind to murine PrP.

FDC-P1 line expresses a significant amount of PrP^{C} and is permissible to infection with 22L strain

FDC-P1 cells have the morphology of lymphocytes and as shown in Fig. 2. This line expresses a substantial amount of PrP^{C}. Anti-PrP immunostaining with Mab 6D11 was localized mainly to the cell membrane (Fig. 2A, B). Confocal microscopy analysis confirmed strong surface localization with little to no non-surface immuno-reactivity (Fig. 2B). Comparison between N2a and FDC-P1 cells performed on Western-blot showed that the amount of PrP^{Sc} in 30 μg of FDC-P1 lysate sample is comparable to that present in 20 μg sample of N2a cell lysate (Fig. 2B). FDC-P1 line expresses all three PrP isoforms with the diglycosylated form being the most abundant.

We successfully infected the FDC-P1 line with the 22L mouse-adapted scrapie strain. As shown in Fig. 3A the presence of PK resistant PrP^{Sc} was detected in a number of sequential passages of FDC-P1/22L cells after infection. Sequential passages of FDC-P1/22L cells did not accumulate PrP^{Sc} in that the rate of cell division proceeded faster than agent replication. A strong PrP^{Sc} signal was consistently seen in the fourth passage after the infection. Its persistence in subsequent passages varied between particular infectivity experiments. No signal was detected in non-infected FDC-P1 cells subjected to PK digestion in a control Western-blot (not shown). As depicted in Fig. 2 no significant differences were evident in the pattern or intensity of anti-PrP immunostaining or the total PrP detected on Western-blot between FDC-P1 and FDC-P1/22L cells. Infection of FDC-P1 line was not associated with changes in cell viability as investigated by MTT assay (Fig. 4C).

In a control experiment, we exposed cells of RAW 264.7 murine macrophage line to the 22L infectious inoculum replicating conditions used to infect FDC-P1 cells. RAW 264.7, similar to FDC-P1 cells are antigen presenting cells capable of phagocytosing the brain inoculum but unable to sustain PrP^{Sc} replication (Luhr et al., 2002). Following infection of RAW 264.7 cells, PrP^{Sc} derived from the inoculum could be detected only in the first passage, and in a very small amount in the second passage (Fig. 3B). This experiment suggests that the strong PrP^{Sc} signal detected in the third and later passages of FDC-P1/22L cells results from de novo conversion of the nascent PrP^{C} to PrP^{Sc} and is not derived from the inoculum.

Mab 6D11 prevents infection of FDC-P1 cells and abrogates the presence of PrP^{Sc} in FDC-P1/22L infected line

The infection of FDC-P1 cells with 22L agent was preventable if performed in the presence of 6D11 Mab. When both the PrP^{Sc} containing inoculum and the FDC-P1 cells prior to infection procedure were preincubated with Mab 6D11 inefficient conversion of PrP^{C} to PrP^{Sc} was observed, which self-extinguished in the second and third passages (Fig. 3C, D). No significant or consistent differences between repeated experiments were observed to indicate that either pre-incubation of cells or inoculum rendered PrP^{Sc} signal disappearance more readily. Murine IgG had no effect on preventing FDC-P1 cell infection (data not shown).

We treated stably-infected FDC-P1/22L cells with various concentrations of Mab 6D11. This treatment resulted in the permanent abrogation of PrP^{Sc} (Fig. 4A). The half of maximal inhibitory concentration (IC_{50}) for 6D11 Mab in the FDC-P1/22L model was calculated from a sigmoidal dose–response curve to be 0.025± 0.01 μg/mL (0.17±0.07 nM; mean± standard deviation from three independent experiment; Fig. 4B). The IC_{50} for Mab 6D11 in stably infected N2a/22L cells was 0.07±0.02 μg/mL (0.47±0.13 nM). FDC-P1 cells that showed abrogation of PrP^{Sc} with effective 6D11 treatment were subsequently cultured in antibody-free medium for up to 14 days without any re-occurrence of PrP^{Sc}. Exposure of FDC-P1 or FDC-P1/22L cells to murine 6D11 Mab or IgG had no statistically significant influence on cell viability (Fig. 4C).

Passive immunization suppresses PrP^{Sc} replicationin the lymphoid organs

Mab 6D11, murine IgG, or vehicle were administered to CD-1 mice following extracerebral scrapie inoculation. No PrP^{Sc} could be detected in spleen homogenates from sentinel mice that received 6D11 treatment and which were sacrificed four weeks after inoculation (Fig. 5A). Among the 6D11 treated mice sacrificed eight weeks after the inoculation, two showed a weak PrP^{Sc} signal detected by HSIBA ((+) 8 wks)); three others were negative ((−)8 wks). Conversely, both IgG and vehicle treated mice showed a strong PrP^{Sc} signal on Western-blot at four weeks post inoculation (Fig. 5A). Strong anti-PrP immunoreactivity in germinal centers of the spleen was detected in these two groups, but not in the 6D11 Mab treated group (Fig. 5B). Despite massive accumulation of PrP^{Sc} in the LRS in control groups, no presence of PrP^{Sc} in the CNS was detected by HSIBA at four and eight weeks after inoculation. This indicates that during the early stage of prion infection the presence of PrP^{Sc} is limited to the extra-CNS tissue where it can be successfully targeted with therapeutically effective anti-PrP Mabs.

Short-term passive immunization significantly increases the incubation period

Starting from 100 days post inoculation (dpi) mice were evaluated weekly using a transverse beam crossing competency test to detect the earliest neurological signs of the CNS involvement. Kaplan–Meier survival analysis demonstrated a statistically significant treatment effect (Fig. 6). The median length of the incubation period in the group treated with Mab 6D11 for four weeks was extended by 58 days (36.9%; p<0.00016D11 vs. IgG and vehicle groups; log–rank test) and the difference between the time the last animal from each group became symptomatic was 81 days. For the eight weeks treatment experiment the difference between median length of incubation periods was 54.5 days (34.7%; pb0.0001 6D11 vs. IgG and vehicle groups log–rank test) and the difference between the longest incubation period was 74 days. There was no statistical difference between groups treated with Mab 6D11 for 4 and 8 weeks. IgG had no effect on the incubation period compared to the vehicle.

Passive immunization ameliorates CNS pathology

All animals were killed when they displayed early neurological symptoms for three consecutive weeks. At this stage mice were capable of walking and feeding themselves without difficulties. Comparison of the PrP^{Sc} level in the CNS by semi-quantitative Western-blot revealed that Mab 6D11 treated mice had 79% less PrP^{Sc} than control CD-1 inoculated with the same batch of 22L inoculum but receiving no injections (cohort infectivity control) and killed at the same stage of early symptomatic disease (one-way ANOVA $p<0.0001$; Tukey-HSD post-hoc test; Fig. 7A, B). The PrP^{Sc} levels in the CNS in groups receiving vehicle or IgG injections were 99% and 98.5% of the value for the control group of CD-1 mice infected with strain 22L, respectively (one-way ANOVA non significant). The differences in the CNS PrP^{Sc} levels between 6D11 treated group and vehicle or IgG groups were statistically significant (one-way ANOVA $p<0.0001$; Tukey-HSD post-hoc test for 6D11 vs. vehicle or IgG $p<0.0001$; Fig. 7A, B). Quantification of the numerical density of spongiform changes in the cingulate cortex revealed significant differences between Mab 6D11 treated mice and mice receiving vehicle or IgG. Mab 6D11 treated mice had 48.4% less spongiform lesions than the vehicle treated group and 44.7% less lesions than IgG treated group (one-way ANOVA $p<0.0001$; Tukey-HSD post-hoc test for 6D11 vs. vehicle or IgG $p<0.0001$; Fig. 7C, D). We also compared the GFAP-reactive astrogliosis, which is not only a general marker of CNS pathology but its level is known to be upregulated early in the course of prion diseases (Stone et al., 2003). Although the level of GFAP in Mab 6D11 treated animals was significantly higher than that in non infected mice (one-way ANOVA $p<0.0001$; Tukey-HSD post-hoc test $p<0.0001$) it was lower by 46.2% compared to the vehicle treated group and by 48.1% compared to the IgG treated group (oneway ANOVA $p<0.0001$; Tukey-HSD post-hoc test for 6D11 vs. vehicle and IgG pb0.0001; Fig. 7E, F). Examination of anti-GFAP stained brain section revealed increased density and hypertrophy of GFAP-positive astrocytes in the 6D11 treated group compared to the normal brain, however the degree of GFAP-reactive astrogliosis in vehicle and IgG treated groups were remarkably greater (Fig. 7G). In contrast to CNS PrP^{Sc} levels, comparison of the PrP^{Sc} level in the spleen homogenates of early symptomatic animals did not reveal any differences among experimental groups, confirming rebound of PrP^{Sc} replication in the LRS following cessation of treatment (Fig. 8).

Discussion

Delay in the secondary spread of infection from the lymphoid cells to the CNS makes passive immunization a viable approach to prevent or delay the CNS involvement and occurrence of neurological symptoms. Previously, the therapeutic potential of anti-PrP Mab was demonstrated using only neural and hypothalamic lines infected with 22L or RML strains (Enari et al., 2001; Pankiewicz et al., 2006; Peretz et al., 2001; Perrier et al., 2004). We are reporting here a new model of in vitro PrP^{Sc} replication in the myeloid precursor line FDC-P1/22L which is relevant to a lymphoid stage of prion infection. Treatment of FDC-P1/22L cells with anti-PrP Mab 6D11 resulted in permanent abrogation of PrP^{Sc} similar to the previously reported abrogation of PrP^{Sc} from the N2a/22L infected neuroblastoma cell line. We have also demonstrated that passive immunization of CD-1 mice with 6D11 Mab, but not with murine IgG, suppresses PrP^{Sc} replication in the LRS. Experience with passive immunization as a therapeutic approach to prevent prion infection, and in particular data on the effectiveness of anti-PrP Mabs on PrP^{Sc} replication on lymphoid cells are limited. Heppner et al. who generated transgenic mice expressing the light chain of 6H4 anti-PrP Mab and then challenged these mice with prion inoculum reported a reduction in PrP^{Sc} content within the lymphoid organs (Heppner et al., 2001). White et al. treated mice with Mab for 500 days following extracerebral inoculation and reported no CNS involvement using continued Mab therapy although residual PrP^{Sc} could be detected in the LRS both by Western-blot and infectivity bioassay (White et al., 2003). The experimental designs in both studies were based

on providing life-long therapy and did not assess the effectiveness of short-time passive immunization. In contrast, our experiment was designed to investigate whether time-limited treatment, which is more clinically feasible than life-long therapy, would be sufficient to eradicate PrP^{Sc} from the LRS and prevent the neurological consequences of prion exposure. Although we showed a substantial effect of systemically administered Mabs on PrP^{Sc} burden in the LRS and extension of the incubation period, time-limited treatment was not capable of preventing the disease. Nevertheless, the results of passive immunization experiments are encouraging and could be significantly improved by identification of the mechanisms responsible for resistance to treatment in vivo. Several explanations can be explored to investigate why anti-PrP Mabs capable of permanent abrogation of PrP^{Sc} from neural cell lines such as 6H4 (Peretz et al., 2001) and 6D11 (Pankiewicz et al., 2006) which is also effective in abrogating PrP^{Sc} from a lymphoid cell line are only partially effective in vivo (Heppner et al., 2001). One explanation could be that various lymphoid cells lines are responsible for spread and maintenance of prion infectivity in vivo and have differential sensitivities to Mabs. Several lineages of lymphoid cells constitutively expressing PrP^{C} (Aucouturier et al., 1999; Mabbott and MacPherson, 2006) form a redundant system in which some lineages may support prion application while others are cleared from infection (Mabbott et al., 2000; Prinz et al., 2002; Weissmann et al., 2001). FDCs occurring in the germinal centers of the spleen and lymph nodes are considered a main source of PrP^{Sc} deposited in the LRS (Brown et al., 1999; Mabbott et al., 2000; Raymond et al., 2007). However, in the absence of functional FDCs the replication of PrP^{Sc} can take place, followed by neuroinvasion albeit with a significant delay (Mabbott et al., 2000; Raymond et al., 2007; Prinz et al., 2002). FDCs are long-lived antigen presenting cells that are not proliferating, making these cells potentially more resistant to antibody treatment than FDC-P1 or other lines which are readily dividing. As it has been shown recently, prion accumulation is inversely proportional to the division rate of cultured cells (Ghaemmaghami et al., 2007) although the relationship between the cell division rate and resistance to treatment has not been established. Since the precursor of FDCs cells is unknown and isolated FDCs cells are poorly renewable in vitro (Park and Choi, 2005) these cells do not constitute a feasible lineage for modeling of prion infection and studying the effect of Mabs in vitro.

The persistence of PrP^{Sc} in cells can also be related to its accumulation in lysosomal vesicles where the acidic pH stabilizes a β-sheet conformation facilitating aggregation, and thus may be less accessible for targeting by Mabs. Although we and others have shown that antibodies in cell culture may be internalized into the lysosomes together with PrP^{Sc}, the effectiveness of this approach may be insufficient in vivo. An alternative mechanism responsible for resistance to treatment in vivo may concern the ability of PrP^{Sc} to form highly infectious PrP^{Sc} aggregates. Silveira et al. (2005) have demonstrated that PrP^{Sc} aggregates of 300–600 kDa that consist of 14–28 PrP molecules are the most virulent prion protein particles. Their virulence is significantly superior to monomeric PrP^{Sc} or larger fibers. Hence, it is possible that a small amount of oligomers escapes the therapeutic effect of Mabs and constitutes a reservoir of reinfection upon cessation of treatment. One or more of these mechanisms may be responsible for the disparity between the in vitro and in vivo treatment results.

Although time-limited passive immunization did not prevent disease, the onset of neurological symptoms was significantly delayed. Accumulation of PrP^{Sc} in the LRS has been shown to be mandatory for subsequent involvement of the CNS (Brown et al.,1999; Mabbott et al., 2000; Raymond et al., 2007), hence its depletion by the anti-PrP Mabs effectively impairs neuroinvasion, delaying the incubation period of the disease. This is a positive clinical result of passive immunization. The proposed pathways of neuroinvasion include the spread of prions via afferent and efferent sympathetic nerve fibers to the spinal cord and/or through the vagus nerve directly to the brain stem (Beekes et al., 1998; Beekes and McBride, 2000; Groschup et al., 1999; McBride and Beekes, 1999). There is also less convincing evidence that

neuroinvasion occurs by direct penetration of the blood-brain-barrier by PrP^{Sc} carrying lymphocytes (Lewicki et al., 2003). Hence PrP^{Sc} can reach the CNS through several autonomic pathways and possibly through the BBB simultaneously, nevertheless the effectiveness of this process is heavily dependent on PrP^{Sc} load on lymphoid cells (Fraser and Dickinson, 1970; Fraser and DiDario, 1978), where it is sensitive to treatment approaches like passive immunization.

It was unexpected to observe that 6D11 treated animals had a reduction of CNS pathology. We noticed not only a decrease in the concentration of PrP^{Sc} and density of spongiform changes but also a reduction in reactive astrocytosis and GFAP up-regulation. It is generally agreed that reactive astrocytosis in prionoses is more intense than would be predicted by the degree of nerve cell loss (Masters and Richardson, 1978). Experiments have shown that astrocyte proliferation and associated GFAP up-regulation are stimulated by aggregates of prion protein (Ironside and Head, 2008). Therefore, GFAP-positive astrocytosis is considered a sensitive marker of prion pathology. Since Mab have limited BBB permeability and the treatment was terminated before the neuroinvasion occurred, the observed results cannot be attributed to direct action of Mabs on PrP^{Sc} replication in the CNS. Therefore, the depletion of PrP^{Sc} level in the lymphoid organs has not only a positive effect on delaying neuroinvasion but also on its effectiveness and subsequent severity of CNS pathology. Since diminution of CNS pathology was unexpected, we did not investigate whether the course of symptomatic disease is altered. However, in light of our observations one may expect that the clinical course of neurological disease in 6D11 treated mice may be prolonged, which could be an additional benefit of passive immunization following prion exposure.

Further development of passive immunization as a therapeutic approach for clinical application requires investigation of the mechanisms responsible for resistance to in vivo treatment, as well as, identification of Mabs effective against replication of human PrP^{Sc}. Thus far the effect of Mabs has been demonstrated only in cell culture and animal models of prionoses, however some identified Mabs, including 6D11 react strongly with human PrP; therefore one may speculate that they will be effective against human diseases as well. Passive administration of humanized anti-PrP Mabs with a high therapeutic potency could be offered to human subjects accidentally exposed to prions in order to delay or even prevent the occurrence of neurological consequences of CNS invasion.

Acknowledgments

This research was supported by Paul B. Beeson Career Development Award in Research on Aging AG24847 (MS), Alzheimer's Association IIRG-08-90630 grant (MS), NIH grants NS47433 (TW), TW006848 (TW), NIH contract N01-NS-02327 (RJK), and an Alzheimer's Association grant (TW).

References

Aucouturier P, Frangione B, Wisniewski T. Prion diseases and the immune system. Ann. Med. Interne 1999;150:75–78.

Aucouturier P, Geissmann F, Damotte D, Saborio GP, Meeker HC, Kascsak R, Kascsak R, Carp RI, Wisniewski T. Infected dendritic cells are sufficient for prion transmission to the CNS in mouse scrapie. J. Clin. Invest 2001;108:703–708. [PubMed: 11544275]

Beekes M, McBride PA. Early accumulation of pathological PrP in the enteric nervous system and gut-associated lymphoid tissue of hamsters orally infected with scrapie. Neurosci. Lett 2000;278:181–184. [PubMed: 10653023]

Beekes M, McBride PA, Baldauf E. Cerebral targeting indicates vagal spread of infection in hamsters fed with scrapie. J. Gen. Virol 1998;3:601–607. [PubMed: 9519840]

Bourette RP, Myles GM, Carlberg K, Chen AR, Rohrschneider LR. Uncoupling of the proliferation and differentiation signals mediated by the murine macrophage colony-stimulating factor receptor expressed in myeloid FDC-P1 cells. Cell Growth Differ 1995;6:631–645. [PubMed: 7545432]

Brown KL, Stewart K, Ritchie DL, Mabbott NA, Williams A, Fraser H, Morrison WI, Bruce ME. Scrapie replication in lymphoid tissues depends on prion protein-expressing follicular dendritic cells. Nature Med 1999;5:1308–1312. [PubMed: 10545999]

Brown P, Brandel JP, Preese M, Sato T. Iatrogenic Creutzfeldt-Jakob disease: the waning of an era. Neurology 2006;67:389–393. [PubMed: 16855204]

Burthem J, Urban B, Pain A, Roberts DJ. The normal cellular prion protein is strongly expressed by myeloid dendritic cells. Blood 2001;98:3733–3738. [PubMed: 11739179]

Carp RI, Callahan SM, Sersen EA, Moretz RC. Preclinical changes in weight of scrapie-infected mice as a function of scrapie agent-mouse strain combination. Intervirology 1984;27:61–69. [PubMed: 6421769]

Dexter TM, Garland J, Scott D, Scolnick E, Metcalf D. Growth of factor-dependent hemopoietic precursor cell lines. J. Exp. Med 1980;152:1036–1047. [PubMed: 6968334]

Eklund CM, Kennedy RC, Hadlow WJ. Pathogenesis of scrapie virus infected mice. J. Infect. Dis 1967;117:15–22. [PubMed: 4961240]

Enari M, Flechsig E, Weissmann C. Scrapie prion protein accumulation by scrapie-infected neuroblastoma cells abrogated by exposure to a prion protein antibody. Proc. Natl. Acad. Sci. U. S. A 2001;98:9295–9299. [PubMed: 11470893]

Feraudet C, Morel N, Simon S, Volland H, Frobert Y, Creminon C, Vilette D, Lehmann S, Grassi J. Screening of 145 anti-PrP monoclonal antibodies for their capacity to inhibit PrPSc replication in infected cells. J. Biol. Chem 2005;280:11247–11258. [PubMed: 15618225]

Fraser H, Dickinson AG. Pathogenesis of scrapie in the mouse: the role of the spleen. Nature 1970;226:462–463. [PubMed: 4985820]

Fraser H, DiDario AG. Studies of the lymphoreticular system in the pathogenesis of scrapie: the role of spleen and thymus. J. Comp. Pathol 1978;88:563–573. [PubMed: 101558]

Ghaemmaghami S, Phuan PW, Perkins B, Ullman J, May BC, Cohen FE, Prusiner SB. Cell division modulates prion accumulation in cultured cells. Proc. Natl. Acad. Sci. U. S. A 2007;104:17971–17976. [PubMed: 17989223]

Goni F, Knudsen EL, Schreiber F, Scholtzova H, Pankiewicz J, Carp RI, Meeker HC, Rubenstein R, Chabalgoity JA, Sigurdsson EM, Wisniewski T. Mucosal vaccination delays or prevents prion infection via an oral route. Neuroscience 2005;133:413–421. [PubMed: 15878645]

Groschup MH, Beekes M, McBride PA, Hardt M, Hainfellner JA, Budka H. Deposition of disease-associated prion protein involves the peripheral nervous system in experimental scrapie. Acta Neuropathol 1999;98:453–457. [PubMed: 10541866]

Heppner FL, Musahl C, Arrighi I, Klein MA, Rulicke T, Oesch B, Zinkernagel RM, Kalinke U, Aguzzi A. Prevention of scrapie pathogenesis by transgenic expression of anti-prion protein antibodies. Science 2001;294:178–182. [PubMed: 11546838]

Hilton DA. Pathogenesis and prevalence of variant Creutzfeldt-Jakob disease. J. Pathol 2006;208:134–141. [PubMed: 16362983]

Hilton DA, Ghani AC, Conyers L, Edwards P, McCardle L, Ritchie D, Penney M, Hegazy D, Ironside JW. Prevalence of lymphoreticular prion protein accumulation in UK tissue samples. J. Pathol 2004a; 203:733–739. [PubMed: 15221931]

Hilton DA, Sutak J, Smith ME, Penney M, Conyers L, Edwards P, McCardle L, Ritchie D, Head MW, Wiley CA, Ironside JW. Specificity of lympho-reticular accumulation of prion protein for variant Creutzfeldt-Jakob disease. J. Clin. Pathol 2004b;57:300–302. [PubMed: 14990604]

Ironside JW, Head MW. Biology and neuropathology of prion diseases. Handb. Clin. Neurol 2008;89:779–797. [PubMed: 18631794]

Jimenez-Huete A, Lievens PMJ, Vidal R, Piccardo P, Ghetti B, Tagliavini F, Frangione B, Prelli F. Endogenous proteolytic cleavage of normal and disease-associated isoforms of the human prion protein in neural and non-neural tissues. Am. J. Pathol 1998;153:1561–1572. [PubMed: 9811348]

Junttila I, Bourette RP, Rohrschneider LR, Silvennoinen O. M-CSF induced differentiation of myeloid precursor cells involves activation of PKC-delta and expression of Pkare. J. Leukoc. Biol 2003;73:281–288. [PubMed: 12554805]

Kascsak RJ, Rubenstein R, Merz PA, Carp RI, Robakis NK, Wisniewski HM, Diringer H. Immunological comparison of scrapie-associated fibrils isolated from animals infected with four different scrapie strains. J. Virol 1986;59:676–683. [PubMed: 2426470]

Kascsak RJ, Rubenstein R, Merz PA, Tonna-DeMasi M, Fersko R, Carp RI, Wisniewski HM, Diringer H. Mouse polyclonal and monoclonal antibody to scrapie-associated fibril proteins. J. Virol 1987;61:3688–3693. [PubMed: 2446004]

Kimberlin RH, Walker CA. The role of the spleen in the neuroinvasion of scrapie in mice. Virus Res 1989;12:201–212. [PubMed: 2499134]

Lewicki H, Tishon A, Homann D, Mazarguil H, Laval F, Asensio VC, Campbell IL, DeArmond S, Coon B, Teng C, Gairin JE, Oldstone MB. Tcells infiltrate the brain in murine and human transmissible spongiform encephalopathies. J. Virol 2003;77:3799–3808. [PubMed: 12610154]

Liu T, Li R, Wong BS, Liu D, Pan T, Petersen RB, Gambetti P, Sy MS. Normal cellular prion protein is preferentially expressed on subpopulations of murine hemopoietic cells. J. Immunol 2001;166:3733–3742. [PubMed: 11238614]

Llewelyn CA, Hewitt PE, Knight RSG, Amar K, Cousens SN, MacKenzie J, Will RG. Possible transmission of variant Creutzfeldt-Jakob disease: overlap of pathogenic mechanisms. Lancet 2004;363:417–421. [PubMed: 14962520]

Luhr KM, Wallin RP, Ljunggren HG, Low P, Taraboulos A, Kristensson K. Processing and degradation of exogenous prion protein by CD11c(+) myeloid dendritic cells in vitro. J. Virol 2002;76:12259–12264. [PubMed: 12414965]

Mabbott NA, Mackay F, Minns F, Bruce ME. Temporary inactivation of follicular dendritic cells delays neuroinvasion of scrapie. Nat. Med 2000;6:719–720. [PubMed: 10888894]

Mabbott NA, MacPherson GG. Prions and their lethal journey to the brain. Nat. Rev. Microbiol 2006;4:201–211. [PubMed: 16462753]

Masters CL, Richardson EP. Sub-acute spongiform encephalopathy (Creutz-feldt-Jakob disease). Nature and progression of spongiform change. Brain 1978;101:333–344. [PubMed: 352478]

McBride PA, Beekes M. Pathological PrP is abundant in sympathetic and sensory ganglia of hamsters fed with scrapie. Neurosci. Lett 1999;265:135–138. [PubMed: 10327187]

Montrasio F, Cozzio A, Flechsig E, Rossi D, Klein MA, Rulicke T, Raeber AJ, Vosshenrich CA, Proft J, Aguzzi A, Weissmann C. B lymphocyte-restricted expression of prion protein does not enable prion replication in prion protein knockout mice. Proc. Natl. Acad. Sci. U. S. A 2001;98:4034–4037. [PubMed: 11274428]

Pankiewicz J, Prelli F, Sy MS, Kascsak RJ, Kascsak RB, Spinner DS, Carp RI, Meeker HC, Sadowski M, Wisniewski T. Clearance and prevention of prion infection in cell culture by anti-PrP antibodies. Eur. J. Neurosci 2006;24:2635–2647. [PubMed: 16817866]

Parizek P, Roeckl C, Weber J, Flechsig E, Aguzzi A, Raeber AJ. Similar turnover and shedding of the cellular prion protein in primary lymphoid and neuronal cells. J. Biol. Chem 2001;276:44627–44632. [PubMed: 11571302]

Park CS, Choi YS. How do follicular dendritic cells interact intimately with B cells in the germinal centre? Immunology 2005;114:2–10. [PubMed: 15606789]

Peden AH, Head MW, Ritchie DL, Bell JE, Ironside JW. Preclinical vCJD after blood transfusion in a PRNP codon 129 heterozygous patient. Lancet 2004;364:527–529. [PubMed: 15302196]

Peretz D, Williamson RA, Kaneko K, Vergara J, Leclerc E, Schmitt-Ulms G, Mehlhorn IR, Legname G, Wormald MR, Rudd PM, Dwek RA, Burton DR, Prusiner SB. Antibodies inhibit prion propagation and clear cell cultures of prion infectivity. Nature 2001;412:739–743. [PubMed: 11507642]

Perrier V, Solassol J, Crozet C, Frobert Y, Mourton-Gilles C, Grassi J, Lehmann S. Anti-PrP antibodies block PrPSc replication in prion-infected cell cultures by accelerating PrPC degradation. J. Neurochem 2004;89:454–463. [PubMed: 15056288]

Porter SR. Prion disease: possible implications for oral health care. J. Am. Dent. Assoc 2003;134:1486–1491. [PubMed: 14664268]

Prinz M, Huber G, Macpherson AJ, Heppner FL, Glatzel M, Eugster HP, Wagner N, Aguzzi A. Oral prion infection requires normal numbers of Peyer's patches but not of enteric lymphocytes. Am. J. Pathol 2003;162:1103–1111. [PubMed: 12651603]

Prinz M, Montrasio F, Klein MA, Schwarz P, Priller J, Odermatt B, Pfeffer K, Aguzzi A. Lymph nodal prion replication and neuroinvasion in mice devoid of follicular dendritic cells. Proc. Natl. Acad. Sci. U. S. A 2002;99:919–924. [PubMed: 11792852]

Prusiner SB. Neurodegenerative diseases and prions. N. Eng. J. Med 2001;344:1516–1526.

Raymond CR, Aucouturier P, Mabbott NA. In vivo depletion of CD11c+ cells impairs scrapie agent neuroinvasion from the intestine. J. Immunol 2007;179:7758–7766. [PubMed: 18025222]

Rubenstein R, Merz PA, Kascsak RJ, Scalici CL, Papini MC, Carp RI, Kimberlin RH. Scrapie-infected spleens: analysis of infectivity, scrapie-associated fibrils, and protease-resistant proteins. J. Infect. Dis 1991;164:29–35. [PubMed: 1676044]

Sadowski M, Pankiewicz J, Scholtzova H, Ripellino JA, Li Y, Schmidt SD, Mathews P, Fryer JD, Holtzman DM, Sigurdsson EM, Wisniewski T. Blocking the apolipoprotein E/β-amyloid interaction reduces β-amyloid toxicity and decreases β-amyloid load in transgenic mice. Am. J. Pathol 2004;165:937–948. [PubMed: 15331417]

Sadowski M, Tang CY, Aguilanldo JG, Carp RI, Wisniewski T. In vivo μMRI signal changes in scrapie infected mice. Neurosci. Lett 2003;345:1–4. [PubMed: 12809974]

Sadowski, M.; Verma, A.; Wisniewski, T. Infectious disease of the nervous system: prion diseases. In: Bradley, WG.; Daroff, RB.; Fenichel, GM.; Jankovic, J., editors. Neurology in Clinical Practice. Elsevier: Philadelphia; 2008. p. 1567-1581.

Safar J, Wille H, Itri V, Groth D, Serban A, Torchia M, Cohen FE, Prusiner SB. Eight prion strains have PrPSc molecules with different conformations. Nat. Med 1998;4:1157–1165. [PubMed: 9771749]

Sigurdsson EM, Brown DR, Daniels M, Kascsak RJ, Kascsak R, Carp RI, Meeker HC, Frangione B, Wisniewski T. Vaccination delays the onset of prion disease in mice. Am. J. Pathol 2002;161:13–17. [PubMed: 12107084]

Sigurdsson EM, Sy MS, Li R, Scholtzova H, Kascsak RJ, Kascsak R, Carp RI, Meeker HC, Frangione B, Wisniewski T. Anti-PrP antibodies for prophylaxis following prion exposure in mice. Neurosci. Lett 2003;336:185–187. [PubMed: 12505623]

Silveira JR, Raymond GJ, Hughson AG, Race RE, Sim VL, Hayes SF, Caughey B. The most infectious prion protein particles. Nature 2005;437:257–261. [PubMed: 16148934]

Spinner DS, Kascsak RB, LaFauci G, Meeker HC, Ye X, Flory MJ, Kim JI, Schuller-Levis GB, Levis WR, Wisniewski T, Carp RI, Kascsak RJ. CpG oligodeoxynucleotide-enhanced humoral immune response and production of antibodies to prion protein PrPSc in mice immunized with 139A scrapie-associated fibrils. J. Leukoc. Biol 2007;14:36–43.

Stone EA, Lin Y, Rosengarten H, Kramer HK, Quartermain D. Emerging evidence for a central epinephrine-innervated alpha(1)-adrenergic system that regulates behavioral activation and is impaired in depression. Neuropsychopharmacology 2003;28:1387–1399. [PubMed: 12813473]

Wadsworth JD, Joiner S, Hill AF, Campbell TA, Desbruslais M, Luthert PJ, Collinge J. Tissue distributionof protease resistant prion proteininvariant Creutzfeldt-Jakob disease using a highly sensitive immunoblotting assay. Lancet 2001;358:171–180. [PubMed: 11476832]

Weissmann C. The state of the prion. Nat. Rev. Microbiol 2004;2:861–871. [PubMed: 15494743]

Weissmann C, Enari M, Klohn PC, Rossi D, Flechsig E. Transmission of prions. J. Infect. Dis 2002;186 (Suppl 2):S157–S165. [PubMed: 12424692]

Weissmann C, Raeber AJ, Montrasio F, Hegyi I, Frigg R, Klein MA, Aguzzi A. Prions and the lymphoreticular system. Philos. Trans. R Soc. Lond. B Biol. Sci 2001;356:177–184. [PubMed: 11260798]

West MJ, Slomianka L, Gundersen HJ. Unbiased stereological estimation of the total number of neurons in the subdivisions of the rat hippocampus using the optical fractionator. Anat. Rec 1991;231:482–497. [PubMed: 1793176]

White AR, Enever P, Tayebl M, Mushens R, Linehan J, Brandner S, Anstee D, Collinge J, Hawke S. Monoclonal antibodies inhibit prion replication and delay the development of prion disease. Nature 2003;422:80–83. [PubMed: 12621436]

Wroe SJ, Pal S, Siddique D, Hyare H, Macfarlane R, Joiner S, Linehan JM, Brandner S, Wadsworth JD, Hewitt P, Collinge J. Clinical presentation and pre-mortem diagnosis of variant Creutzfeldt-Jakob disease associated with blood transfusion: a case report. Lancet 2006;368:2061–2067. [PubMed: 17161728]

Zanusso G, Liu D, Ferrari S, Hegyi I, Yin X, Aguzzi A, Hornemann S, Liemann S, Glockshuber R, Manson JC, Brown P, Petersen RB, Gambetti P, Sy MS. Prion protein expression in different species: analysis with a panel of new mAbs. Proc. Natl. Acad. Sci. U. S. A 1998;95:8812–8816. [PubMed: 9671761]

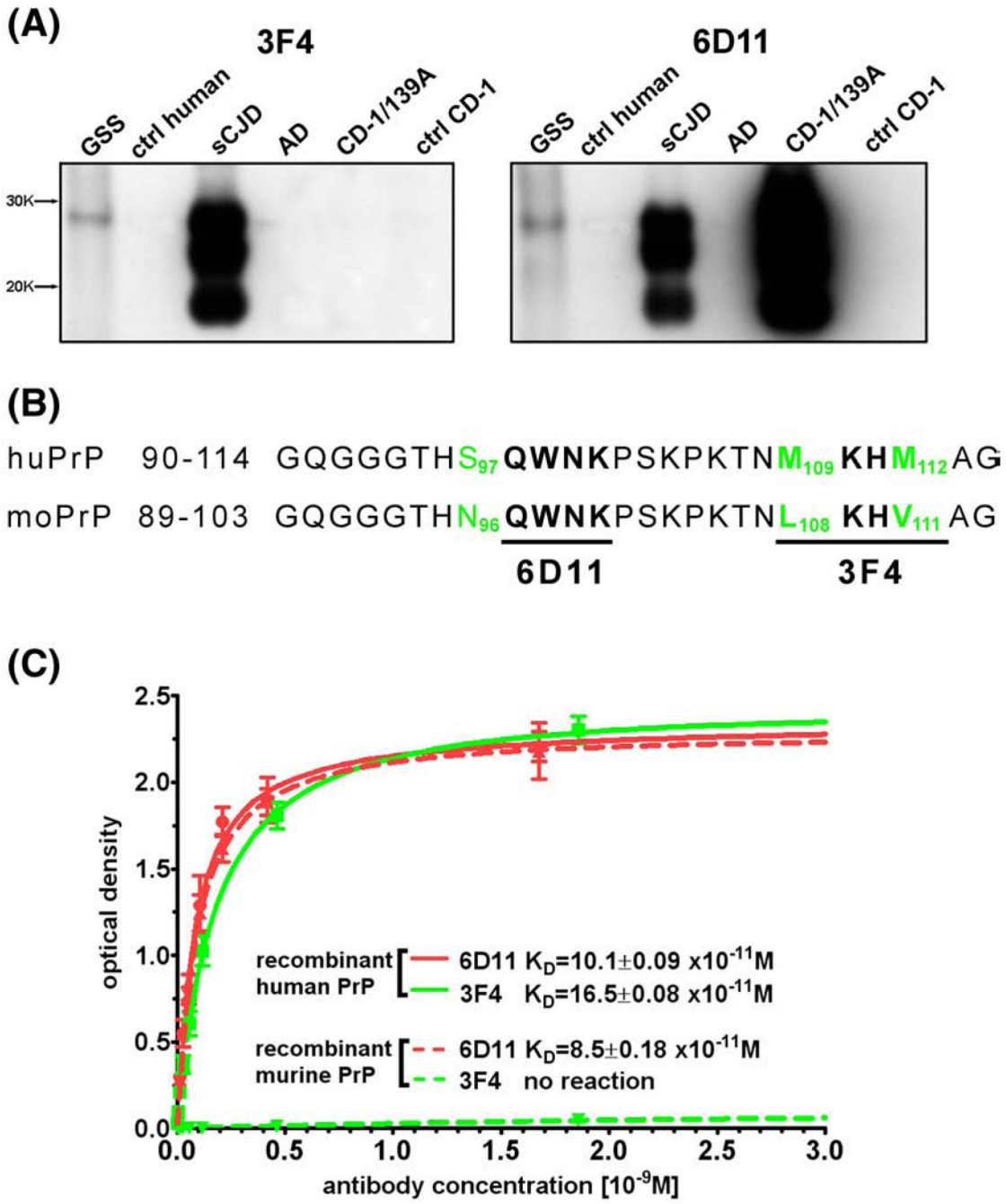

Fig. 1.

Characteristics of Mab 6D11. Mab 6D11 recognizes both human and murine PrP^{Sc}. (A) Shownis a comparison between the reactivity of 3F4 and 6D11 Mabs. Corresponding lanes represent PK digested brain homogenate from a: 1) GSS syndrome patient, 2) control human, 3) sporadic CJD, 4) AD patient, 5) CD-1 mouse infected with 139A mouse adapted scrapie strain, and 6) control mouse. (B) Comparison of homologous epitopes between sequences of murine and human PrP. 6D11 recognizes residues 97–100 of murine PrP (QWNK) which is homologous to sequence 98–101 of the human PrP. 3F4 recognizes residues 109–112 of human PrP (MKHM) but not homologous sequence of murine PrP (LKHV). The numbering of murine residues is shifted by one because murine PrP sequence lacks glycine in position 55. (C) Shown

is a comparison of between binding affinities of 6D11 and 3F4 to human and murine recombinant PrP. Abbreviations: GSS—Gerstmann–Sträussler–Scheinker syndrome, ctrl hum —control human, sCJD—sporadic Creutzfeldt–Jakob disease, AD— Alzheimer's disease, CD —1/139A-CD-1 mouse infected with 139A mouse adapted scrapie strain, and ctrl-CD-1— control CD-1 mouse.

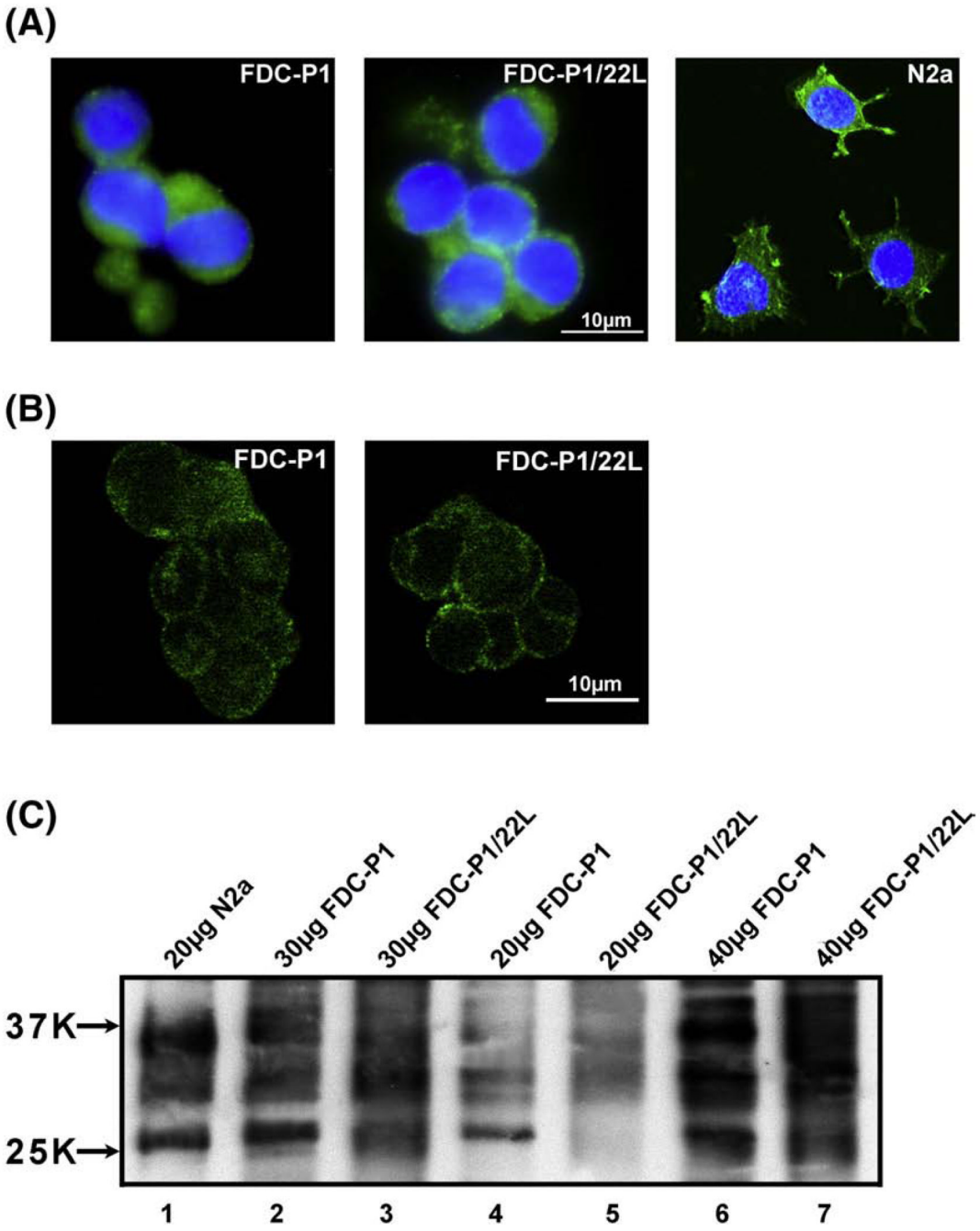

Fig. 2.

FDCs-P1 expresses a significant amount of PrP^{C}. (A) Shown is the morphology and PrP expression in FDC-P1 and FDC-P1/22L cells. PrP expression in N2a murine neuroblastoma cells is shown for comparison. Cells were stained with 6D11 anti-PrP Mab (green) and counterstained with DAPI (blue). (B) Shown are confocal microscopy images (0.2 μm layer thickness) of FDC-P1 and FDC-P1/22L immunostained with 6D11 anti-PrP Mab. Anti-PrP immunoreactivity is primarily localized to the plasma membrane. No significant differences in staining intensity between non-infected and infected FDC-P1 cells were observed. (C) Shown is a comparison of the PrP content in cell lysates of N2a, FDC-P1 and FDC-P1/22L cells. Lane 1 represents N2a cells, lanes 2, 4, 6 FDC-P1 cells, and lanes 3, 5, 7 FDC-P1/22L

cells. 20 μg of total protein was loaded in lanes 1, 4, 5; 30 μg in lanes 2 and 3 and 40 μg in lanes 6 and 7. Lysates from FDC-P1/22L cells were not PK digested. FDC-P1 cells express all three PrP isoforms with the diglycosylated form being the most abundant. The intensity of staining of 30 μg FDC-P1 and FDC-P1/22L samples (lanes 2 and 3) was comparable to that of 20 μg sample of N2a cell lysates (lane 1). No significant differences in the amount of total PrP between FDC-P1 and FDC-P1/22L lines were observed.

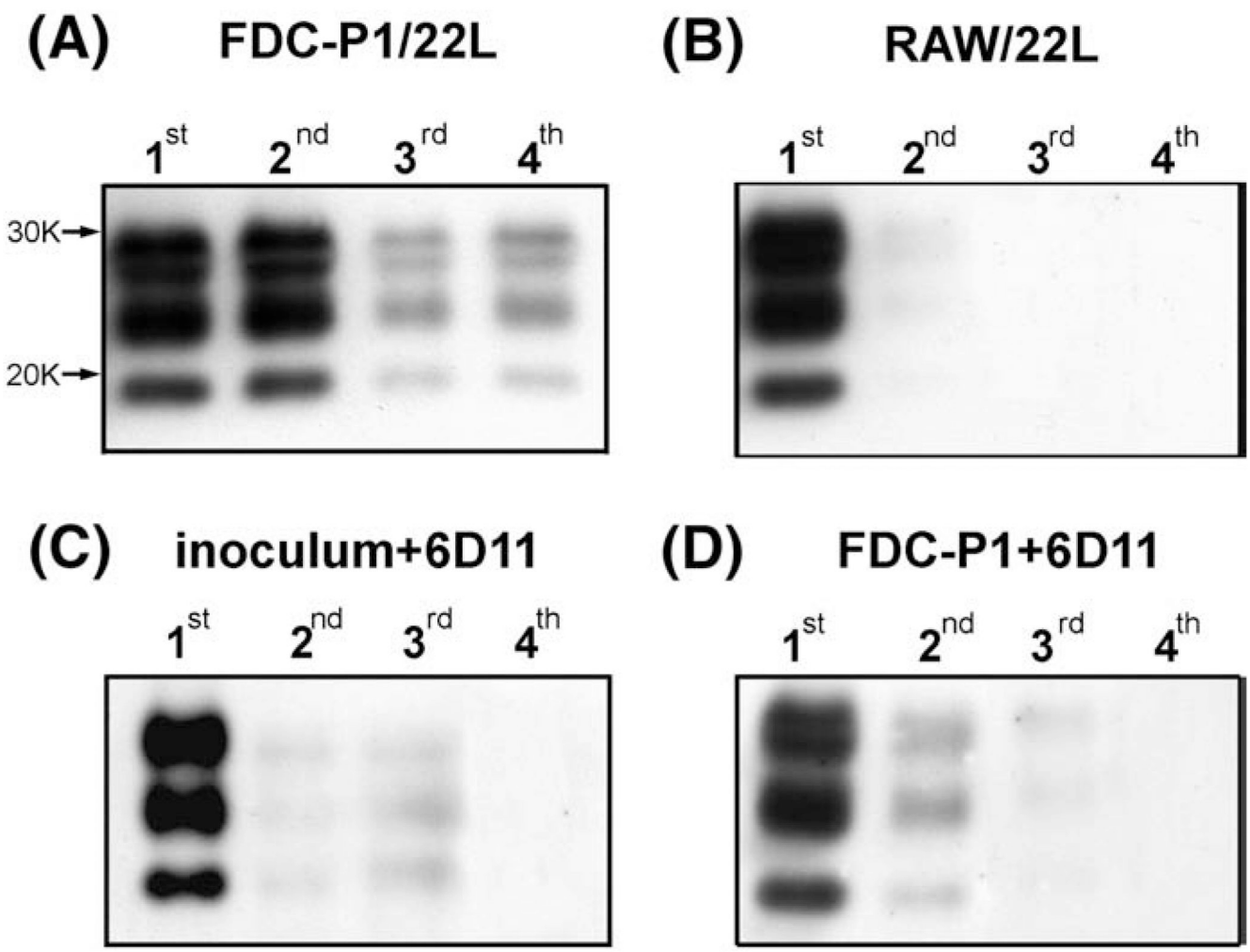

Fig. 3.

FDC-P1 cells are susceptible to infection with 22L strain in vitro and the infection can be prevented using 6D11 Mab. (A) Shown is a Western-blot of PK resistant PrP^{Sc} in passages 1–4 of FDC-P1 cells following infection with 22L strain. The presence of PK resistant material in passages 3 and 4 indicates the ability of FDC-P1 cells to sustain reproduction of PrP^{Sc} in vitro. (B) Shown are RAW cells (a macrophage line) that were exposed to PrP^{Sc} as a control experiment. These cells are able to phagocytize the inoculum but are unable to sustain de novo PrP^{Sc} replication, therefore PrP^{Sc} can be detected only in the first and partially in the second passage. (C) and (D) demonstrate the ability of Mab 6D11 to prevent infection of FDC-P1 line. In (C) the 22L inoculum was incubated with Mab 6D11 prior to infecting FDC-P1 cells, whereas in (D) FDC-P1 cells were incubated with Mab 6D11 prior to adding the 22L inoculum. Both types of intervention prevented effective infection since no PrP^{Sc} is detectable beyond passage 3.

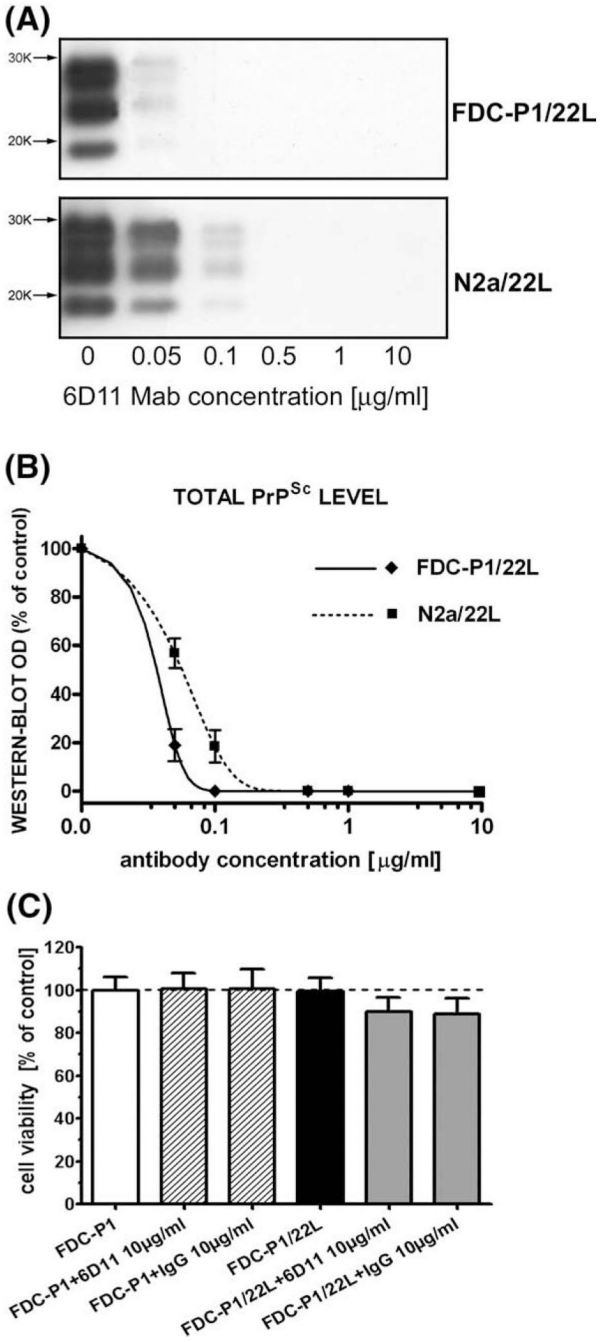

Fig. 4.

Mab 6D11 abrogates the presence of PrP^{Sc} from N2a/22L and FDC-P1/22L infected cell lines without toxicity. (A) Shown are Western-blots of PK treated cell lysates from N2a/22L cells treated for 96 h with different concentrations of Mab. (B) Shown are densitometric measurements of PrP^{Sc} bands detected in the Western-blots and fitted in the sigmoidal dose–response curve. (C) Shown is MTTcytotoxicity assay on infected FDC-P1/22L cells. Neither infection of FDC-P1 line with 22L strain nor treatment of FDC-P1 or FDC-P1/22L lines with 6D11 or murine IgG produced significant decrease in cell viability as assessed by standard MTT cell viability assay. Values in (B) and (C) are given as a mean ± standard deviation from at least three independent experiments.

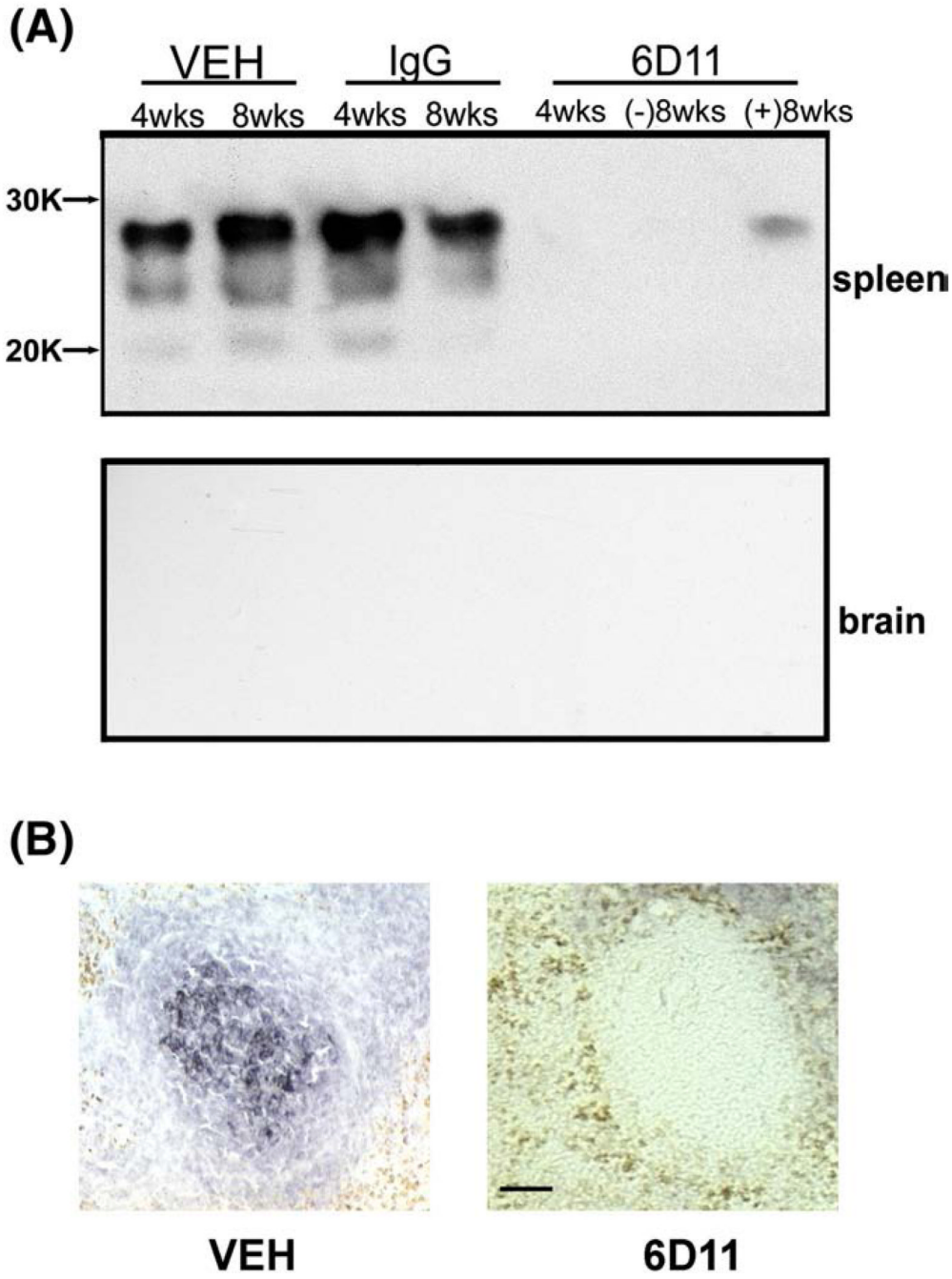

Fig. 5.

Systemic administration of 6D11 Mab inhibits replication of PrP^{Sc} in the LRS. (A) Shown is a highly sensitive immunoblotting assay used for detection of PrP^{Sc} in the spleen and the brain in sentinel mice sacrificed immediately after cessation of treatment. A substantial amount of PrP^{Sc} was detected in spleens of animals treated with vehicle or IgG that were sacrificed four or eight weeks after inoculation. No animal that received Mab 6D11 and was sacrificed four weeks after the inoculation was positive. Three out of five 6D11 treated animals were negative eight weeks after the inoculation ((−)8 wks), and the remaining two showed a faint signal ((+) 8 wks). No animals showed the presence of PrP^{Sc} in the CNS eight weeks after the inoculation indicating that although PrP^{Sc} reaches a high concentration in the LRS there is no CNS

involvement at that stage of infection. (B) Anti-PrP immunohistochemistry. Shown is accumulation of PrP^{Sc} in the germinal zone of the spleen in vehicle treated mice eight weeks after the inoculation. No PrP^{Sc} signal could be detected in Mab 6D11 treated mice at the matched time after inoculation. Scale bar 50 μm. Abbreviation: VEH—vehicle.

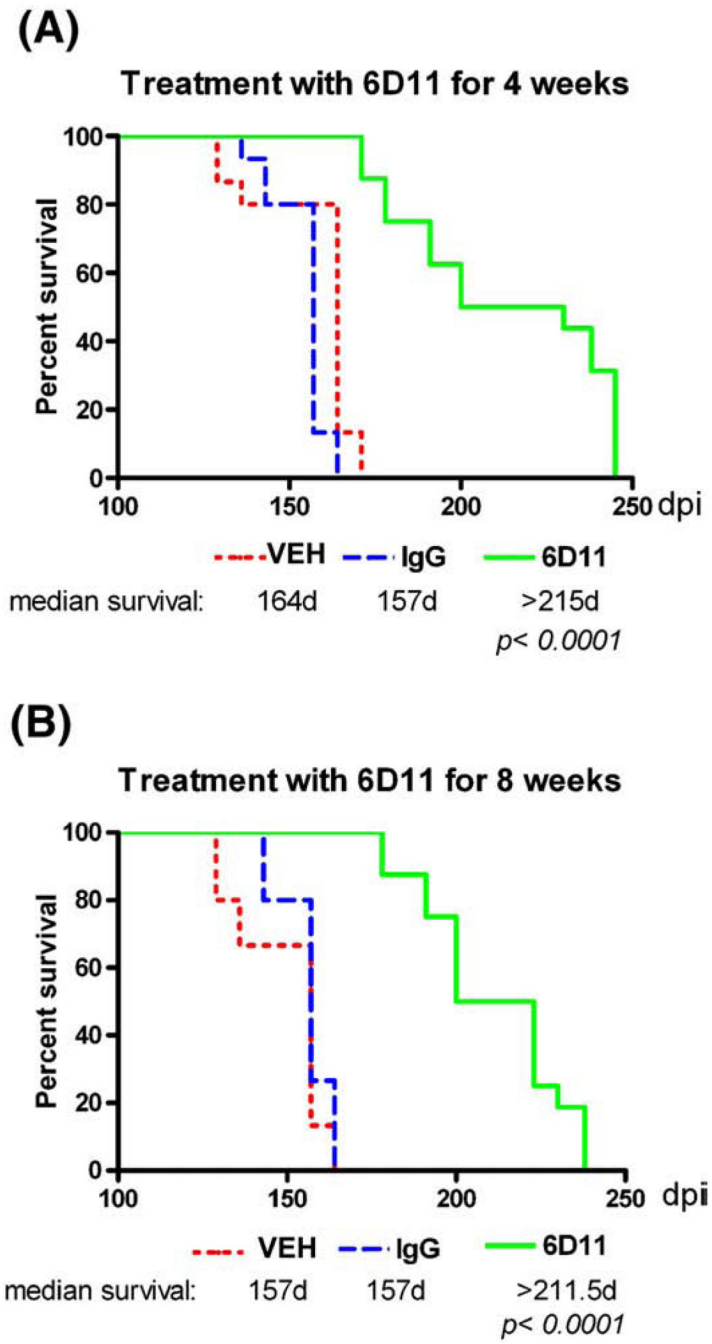

Fig. 6.

Short-term passive immunization delays the onset of neurological symptoms. Shown is a Kaplan–Meier analysis of the incubation time in CD-1 mice that were intraperitoneallyinfected with 22L strain and received treatment with 6D11 for (A) four or (B) eight weeks. A significant delay in onset of symptoms compared to the vehicle and IgG treated groups was observed in both experiments ($p < 0.0001$, log–rank test). Abbreviation: VEH—vehicle.

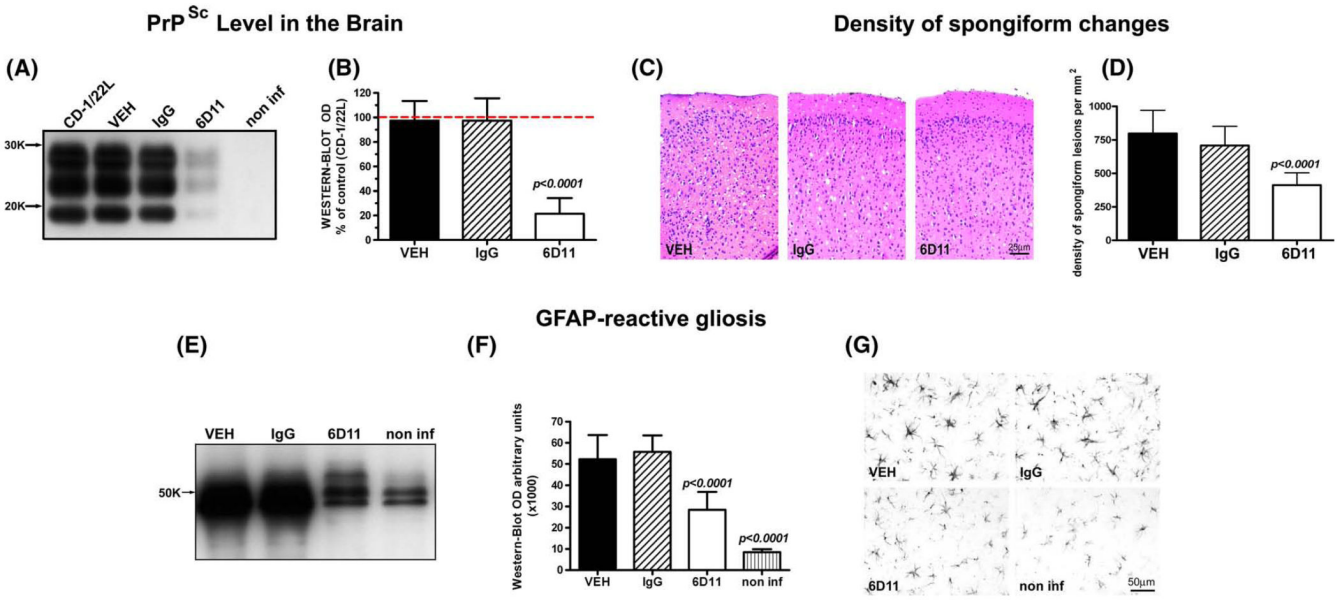

Fig. 7.

Short-term passive immunization has aneffecton CNS pathology. (A) and (B) show a significant reduction in PrP^{Sc} level in the CNS by semi-quantitative Western-blot. Values in (B) are expressed as a percentage of PrP^{Sc} level in the brain of CD-1 mice infected with 22L strain, which received no injections. Differences between 6D11 treated mice and 22L infected control mice, mice treated with vehicle or IgG were statistically significant as indicated. (C) shows representative hematoxylin and eosin stained cortical sections where reduced spongiform changes are evident in the 6D11 treated mice. (D) shows the reduction in the numerical density of spongiform lesions in the brain cortex in 6D11 treated mice. Differences between 6D11 treated mice, and mice treated with vehicle or IgG were statistically significant as indicated. Differences between mice treated with vehicle and IgG were not statistically significant. (E) and (F) show a significant reduction in GFAP level by semi-quantitative Western-blot. Differences between 6D11 treated mice, and mice treated with vehicle or IgG were statistically significant as indicated. Differences between GFAP level in non-infected mice and all other treatment groups (including 6D11) were significant as indicated. Differences in the GFAP level were associated with less activation of astrocytes as seen in (G) in representative GFAP immunohistochemically stained sections. Values in graphs (B), (D), and (F) are displayed as the mean ± standard deviation. Shown p values are for Tukey-HSD post-hoc test. Abbreviations: CD-1/22L—CD-1 mouse infected with 22L strain, non-inf—non infected, GFAP—glial fibrillary acidic protein, and VEH—vehicle.

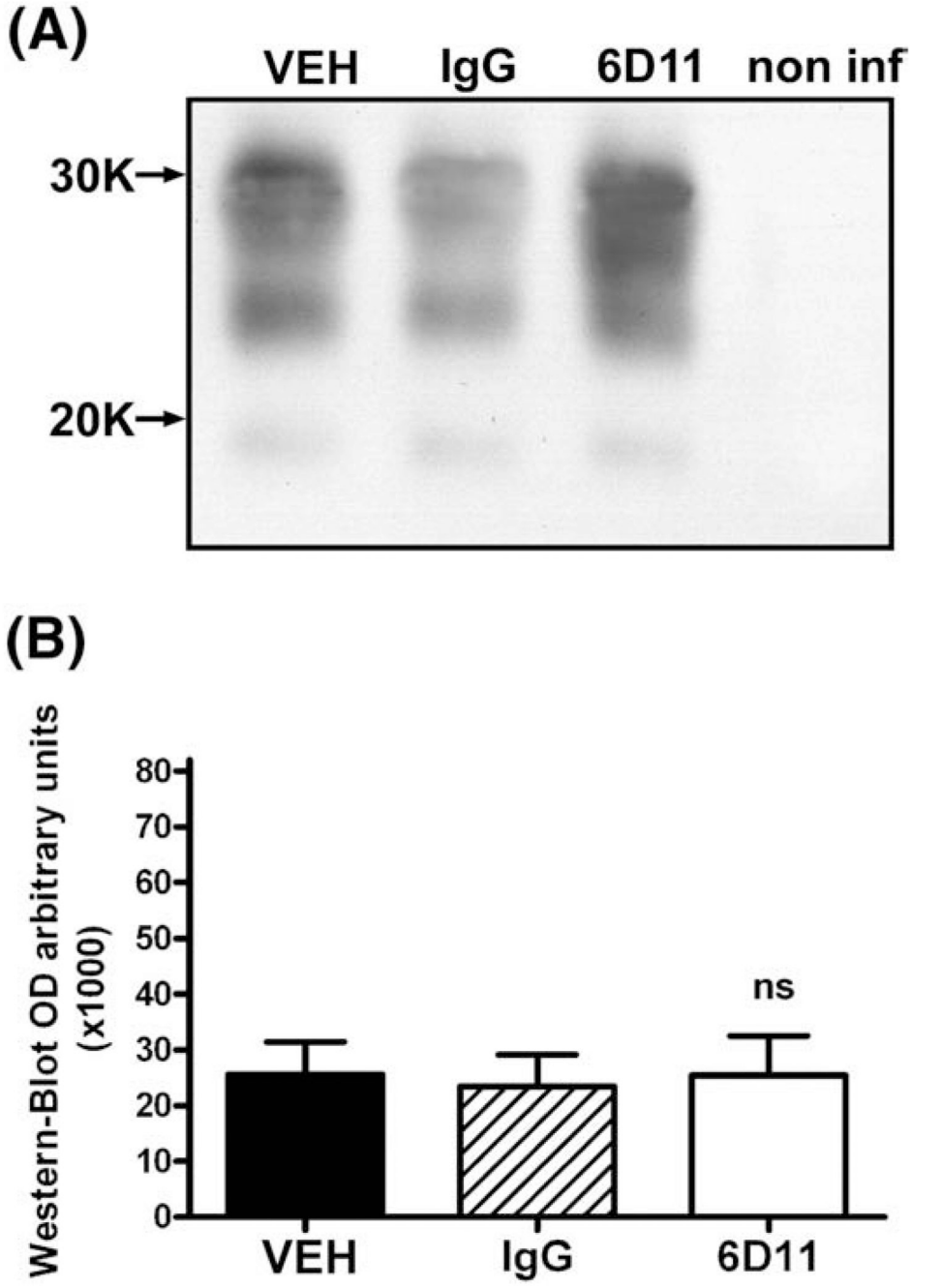

Fig. 8.

The levels of PrP^{Sc} in the spleen did not differ significantly in control and 6D11 treated infected animals when they were killed after displaying neurological symptoms for three weeks in a row. Shown are (A) a Western-blot and (B) results of densitometric analysis of the PrP^{Sc} load in the spleen. No significant differences between 6D11 treated and control infected groups were detected. In (A) a non-infected spleen control is included to document the complete digestion of PrP^{C} by PK treatment. Abbreviations: VEH—vehicle, non inf—non-infected, and PK—proteinase K.